Roadside vehicle particulate matter concentration estimation using artificial neural network model in Addis Ababa, Ethiopia

Solomon Neway Jida, Jean-François Hetet, Pascal Chesse, Awoke Guadie

Roadside vehicle particulate matter concentration estimation using artificial neural network model in Addis Ababa, Ethiopia

Solomon Neway Jida[1, 2*], Jean-François Hetet[1], Pascal Chesse[1], Awoke Guadie[3, 4]

1. Research Laboratory in Hydrodynamics, Energetics & Atmospheric Environment (LHEEA), École Centrale de Nantes. Nantes, 44300, France
2. Department of Mechanical Engineering, Faculty of Mechanical & Production Engineering, Institute of Technology, Arba Minch University, Arba Minch 21, Ethiopia
3. Key Laboratory of Environmental Biotechnology Research Center for Eco-Environmental Sciences, Chinese Academy of Sciences, Beijing 100085, PR China
4. Department of Biology, College of Natural Sciences, Arba Minch University, Arba Minch 21, Ethiopia

Abstract

Currently, vehicle-related particulate matter is the main determinant air pollution in the urban environment. This study was designed to investigate the level of fine ($PM_{2.5}$) and coarse particle (PM_{10}) concentration of roadside vehicles in Addis Ababa, the capital city of Ethiopia using artificial neural network model. To train, test and validate the model, the traffic volume, weather data and particulate matter concentrations were collected from 15 different sites in the city. The experimental results showed that the city average 24-hr $PM_{2.5}$ concentration is 13%-144% and 58%-241% higher than air quality index (AQI) and world health organization (WHO) standards, respectively. The PM_{10} results also exceeded the AQI (54%-65%) and WHO (8%-395%) standards. The model runs using the Levenberg-Marquardt (Trainlm) and the Scaled Conjugate Gradient (Trainscg) and comparison were performed, to identify the minimum fractional error between the observed and the predicted value. The two models were determined using the correlation coefficient and other statistical parameters. The Trainscg model, the average concentration of $PM_{2.5}$ and PM_{10} exhaust emission correlation coefficient were predicted to be (R^2 = 0.775) and (R^2 = 0.92), respectively. The Trainlm model has also well predicted the exhaust emission of $PM_{2.5}$ (R^2 = 0.943) and PM_{10} (R^2 = 0.959). The overall results showed that a better correlation coefficient obtained in the Trainlm model, could be considered as optional methods to predict transport-related particulate matter concentration emission using traffic volume and weather data for Ethiopia cities and other countries that have similar geographical and development settings.

Keywords: Addis Ababa; Artificial neural network; PM prediction; Roadside emission

*Corresponding author. E-mail: solomonnewayjida@gmail.com (Solomon Neway Jida).

Introduction

Transport-related particulate matters (PM) emission can be directly emitted from vehicle exhaust or non-exhaust particles arise from vehicles-related sources. Transport vehicles are the main cause of high PM emission concentration in the urban zones (Gu et al., 2019; Pant and Harrison, 2013). The particle emitted from the vehicle tailpipe (exhaust emission) is influenced by fuel property, oil consumption, fuel introduction mechanism, combustion process, engine size, road gradient, driving condition, and mileage of the vehicles (Watson et al., 1988). Non-exhaust particulate matter also originated from the wear of tyre and road surface, corrosion, and the re-suspension of road dust particles (Garg et al., 2000; Penkała et al., 2018). The growth in traffic volume in cities has led to more traffic jams, rising vehicular accidents, and air pollution (Ngo et al., 2019; Xue et al., 2013). In this sector, the non-exhaust emission contributes around 90% of PM_{10} and 85% of $PM_{2.5}$ emission to the urban background (Timmers and Achten, 2016).

For estimating health adverse effects and monitoring purpose, PM has been well documented and often categorized into $PM_{2.5}$ and PM_{10} (Pope and Dockery, 1992; Fan et al., 2009). The classification of PM is based on aerodynamic diameter, which represents a particle that has less than 2.5 µm (fine particles) and 10 µm (coarse particles) (US EPA, 2016). These particles derived in many sizes, shapes and can be formed hundreds of different chemicals. Furthermore, this challenging the selection step of appropriate monitoring equipment for a researcher in this field of study (Amaral et al., 2015). Although a number of studies exist on PM, the detail health risk due to non-exhaust emissions are not yet perfectly understood (Padoan and Amato, 2018; Stafoggia and Faustini, 2018). In most exhaust PM emissions cases, $PM_{2.5}$ are often considered which comprise a collection of polycyclic aromatic hydrocarbons that affect cardiovascular and breathing system that leads to premature death (Habeebullah, 2013). PM_{10} emission contraction from transport-related mostly categorized under non-exhaust portions, but a little portion of the emission encloses to $PM_{2.5.}$ The formation and concentration level of non-exhaust PM_{10} emission are differ based on sources, however they commonly pretend from heavy metals such as zinc, iron, copper, and lead (Pant and Harrison, 2013). Numerous epidemiological

studies also concluded that exposure to high concentrations of $PM_{2.5}$ and PM_{10} can lead to several health impacts ranging from coughing to premature death (Pope and Dockery, 1992; Fan et al., 2009). Besides, these particles seriously affect the surrounding environment as well as the globe (Park et al., 2018; Mukherjee and Agrawal, 2018). A recent global study showed that, $PM_{2.5}$ accounts about 4.2 million deaths and the fifth risk factor among all worldwide death factors, including smoking, diet, and high blood pressure (Hamanaka and Mutlu, 2018). Besides, many research papers specify that air pollution aggravate the rate of cardiovascular disease and stroke of human health (Fan et al., 2009).

In Ethiopia, air pollution research is still at its infant stage. It is generally assumed that the concentrations of air pollution in Ethiopia is low (Tefera et al., 2016). However, few studies done in different parts of the country indicates that air pollution is progressively becoming a health concern due to high concentrations of indoor, outdoor and other ambient air pollutant emissions (Tarekegn and Gulilat, 2018; Keil et al., 2010). Current national situational analysis and needs assessment report disclosed that health and environment linkage has a weak relationship. However, the report have been pinpointing air pollution as one of the important policy priorities in Ethiopia (Mitike et al., 2016).

Modern motor vehicles are equipped with different air pollution control technologies (Winkler et al., 2018). Despite the advances in car emissions control technologies, for both diesel and gasoline engines, vehicular pollution is quiet a vital concern in air pollution in the urban background. To test emission levels, there are numerous methods such as dynamometer test and real-world driving emission test. Dynamometer test design to detect the emission concentration of an engine during vehicles under stationary position without considering real time traffic flow, a vehicle cumulative mileage, load, road condition, and engine capacity (Hung-Lung and Yao-Sheng, 2009). However, real-world driving emission test measurements have a more representative way to record the series of variability in driver behavior, communication with other road users and infrastructure. As Ropkins and his team stated that, this can be achieved an all-inclusive serious review of the techniques applied to monitor real-world vehicle exhaust emissions (Ropkins et al., 2009). Monitoring of particle concentrations through portable emissions measurement system (PEMS) is an essential activity because data gathering by itself is time-consuming and expensive related to the cost of the monitoring instruments and experimental campaign and reconnaissance of air quality standards also vital (Ngo et al., 2019). Thus, it is challenging for a researcher from a developing country like Ethiopia to contribute a research output in this area. However, various modeling methods can be used as an alternative option to estimate the status of vehicular pollution.

Numerous previous studies indicated that artificial neural networking (ANN) is an influential and useful modelling tool that can recognize the complex relationships from input-output data (Cirak and Demirtas, 2014; Meiller, 1991; Cabaneros et al., 2019). Among the ANN, the multilayer perceptron neural networks model have more capable to predict than traditional multiple regression models (Cabaneros et al., 2019; Gardner and Dorling, 1999). Aydin and co-workers has compared Trainlm and Trainscg algorithm, which is a broadly used training algorithm for multilayer perceptron regression models of multilayer neural network, and they concluded that the Levenberg Marquardt algorithm has a better forecast correlation coefficient performance than scaled conjugate gradient algorithm (Aydin et al., 2018).

In this study, since the relationship between PM ($PM_{2.5}$ and PM_{10}), concentrations with weather and traffic volume data are complex and non-linear, an artificial neural networks model is selected as a potential model that predicts hourly $PM_{2.5}$ and PM_{10} concentrations. Experimental real-time PM pollutant concentration data were collected from 15 sites for 24 hr in Addis Ababa city, road traffic corridors using a portable emission monitor. Thereafter, traffic data and meteorological data were gathered from respective office and online access for the specific dates and areas. Since, Ethiopia doesn't have any emission standard limits for vehicular exhaust pollutant, the output is only compared with the U.S. Environmental Protection Agency (EPA) Air Quality Index (AQI), and World Health Organization (WHO) standards. Moreover, the proposed ANN modelling predicts the output of the system as long as enough experimental data for training, validating and testing.

1. Material and methods

1.1. Study area

Addis Ababa is the political, economic, and industrial center of Ethiopia that covers 527 square kilometers of area. It is located at 9°01'29.89" North latitude, and 38°44'48.80" East longitude, and has 10 sub-cities. It has approximately 6.5 million residents, and its altitude reaches around 2800 m above from sea level (Kume et al., 2010). Vehicle ownership demand in Ethiopia shows a vast increment with time. Among the total number of vehicles in the country, 62% are being used in Addis Ababa and it is believed that this has contributed to high pollution. Besides; research has reported acute upper respiratory infection and unspecified diseases highly increased through time and the amount of carbon dioxide, carbon monoxide, nitrogen, and other toxic gases has increased in and around the city (Tarekegn and Gulilat, 2018; Kume et al., 2010).

The experimental test was performed from 15 sites of Addis Ababa city between October 16 and November 23, 2018. To collect data the apparatus was mounted one meter far from the roadside and 1.5 m above the ground considering the wind direction on each selected road in a 1-minute interval for 24 hr. Some of the monitoring sites and apparatus setup is shown in Fig. 1.

1.2. Data collection techniques

Roadside pollutant emissions concentration data were collected using Aeroqual series-500 digital analyzer. The series 500-air quality monitor is an optical particle counter instrument that has a portable air quality monitor and the sensor head worked in a range of 1-1000 $\mu g/m^3$ with an accuracy of ± 5 $\mu g/m^3$ (Air Quality Sensor, 2018). This apparatus is designed for portable emission measurement that can measure simultaneously $PM_{2.5}$, PM_{10}, relative humidity, and temperature.

A traffic census, by manual counting, was conducted in the study area at a 4-hr interval for 24 hr in all sites. In addition, secondary data were gathered for a few stations from the Addis Ababa traffic management office. Weather-related data as relative humidity and temperature were measured simultaneously every minute. Besides, weather data, including wind speed and wind direction above 10 m from the ground, temperature, and relative humidity for the selected area were extracted from meteoblue online access.

1.3. Artificial neural network models

The ANNs are powerful modelling algorithm for non-linear relationships and can be trained to perfectly simplify when offered with new and fresh data (Maier et al., 2010). The ANN learns to model a relationship during a supervised training technique when they are frequently presented with a series of inputs and related output data. The ANN model is a mathematical model inspired by the biological neurons (Cirak and Demirtas, 2014), and are used to compute a complex and non-linear function. ANN is an effective optional statistical technique for predicting time series (Gardner and Dorling, 1999). The objectives of the prediction models are to bargain the unidentified functional connection between *W* and *X*, the relations in the input vectors in *X* to output vectors in *Y* (Fig. 2) using an activation function (Gardner and Dorling, 1998). The forecasting capability of ANNs outcomes from training in experimental data and following validation with unseen data (Park et al., 2018; Coudray et al., 2009). Each neuron contains x_1, x_2, x_n inputs added to a weight w_{ij} that designates the link interaction of a certain input for each linking, weight bias, and activation function.

The ANN models are general estimators with the capacity to simplify with learning non-linear associations between inputs and output variables. The ANN is interrelated dealt out elements known as neurons that are ordered in layers, which contains inputs, one or more hidden and output layers (Fig. 3). They are connected to each other with neuron or nodes to the next layer and the inputs multiplied by the corresponding weight of the neuron linking based on its virtual importance before entering the hidden layer (Cirak and Demirtas, 2014). The data transfer is permitted only to the next sequential layer. Each node of the hidden layer accepts the arriving signals from the nodes of the input layer. The total input indicator is calculated followings Eqs. (1) and (2):

$$u_i = \sum_{j=1}^{N} W_{ij} X_j + b_i \quad (1)$$

$$y_i = f(u_i) \quad (2)$$

1.4. Model architecture

In this study, the Trainlm and Trainscg algorithm for MLP neural network learning is offered and selected based on their prediction performance of concentrations of $PM_{2.5}$ and PM_{10} for the input data. The Trainlm algorithm is often used ANN model architecture applied for supervised learning problems and was found in a highly accurate recognition ratio of prediction (Suratgar et al., 2007).

Experimental results acquired from the field measurement were used to train, validate, and test the ANN model. Using sigmoid symmetric activation function via Trainlm and Trainscg algorithm technique, the predictive value is associated with the measured value. Finally, the outcomes acquired from the ANN model based on their statistical conformity, especially, the correlation coefficient ($\underline{R}$) between the targets and the output values, show which algorithm works best in ANN. In this work, an MLP holding five input layers, six hidden layers, and a single output layer. For comparison, the back-propagation algorithm with an adaptive learning rate is designated as a standard neural network training method (Kermani et al., 2005). The overview of the model architecture is shown as follow in Fig. 3.

1.5. Inputs variable selection

Selecting the input variable is an important step to develop an ANN model. Hence, the input selection procedure considers the significance of the input that should be justified using an Adhoc approach based on prior information by considering the fact and available data. Road transport emissions are commonly interrelated to the traffic flow, vehicle fuel category, road gradient, and weather condition. Generally, for this work, the input variables are traffic volume, hourly mean temperature, humidity, wind speed, wind direction and PM concentrations.

In this work, feed-forward learning algorithm was used and data are categorized into two parts, for train the network 70% of the data was consumed and the remaining portion for testing and validation of the network. Afterwards distinct train of the networks, the performance of the model checked using since 24-hr data from 4-sites in the city. The models developed in this work used the same input data for a specific site in both cases. However, the model did not use the same input data for all sites because the input data varied from site to site based on their weather and traffic volume recorded.

1.6. Data assurance

To get quality data, the accuracy of the monitoring tool and methods of data collection affected the result. To assure this, the data collector continuously supervised the instrument on the spot. The accuracy of the monitor was crosschecked periodically with the same monitor borrowed from the Ministry of forest, environment, and climate change. To confirm the accuracy of the meteorological data additional weather data were also mined from meteoblue.

The input data must fully specify circumstances about which the network is essential to generalize. To minimize over-training the networks, it is required to split the data into three parts a training, validation and test set. The training step consumes a majority of the data. The validation and test step were used to confirm the overall performance of the trained model. Training can be a pause when the performance of the validation data approach to one. In this work, the models were trained using 70% of the collected data and the remaining 30% were used for testing and validating the model. The details of quality assurance and workflow in this work are shown in Fig. 4.

1.7. Evaluation performance of the model

The efficiency of the ANN models was assessed through the following arithmetical performance indicators; RMSE: the root mean square error, MAE: the mean absolute error, MSE: the mean square error, R^2: correlation coefficient, MB: the mean bias, CRMSE: the centered root mean squared error, MEF: the model efficiency and FB: the fractional bias defined (Eqs. (3)-(10)).

The RMSE (Eq. (3)) was commonly used for further evaluation of the ANN model using outstanding error among the measured and forecasted values to view the universal dissimilarity the two values (Paas et al., 2017).

$$\mathrm{RMSE} = \frac{1}{\mathrm{N}}\sqrt{\sum_{\mathrm{i=1}}^{\mathrm{N}}\left(\mathrm{C_p} - \mathrm{C_m}\right)^2} \qquad (3)$$

The MAE (Eq. (4)) measures the deviation of predicted versus the measured value where all individual differences have equal weight without considering their direction. (Paas et al., 2017).

$$\mathrm{MAE} = \frac{1}{\mathrm{N}}\sum_{\mathrm{i=1}}^{\mathrm{N}}\left|\mathrm{c_p} - \mathrm{c_m}\right| \qquad (4)$$

The MSE (Eq. (5)) is the mean square deviation that the mean scores between the prediction and actual values (Paas et al., 2017).

$$\mathrm{MSE} = \frac{1}{\mathrm{N}}\sum_{\mathrm{i=1}}^{\mathrm{N}}\left|\mathrm{c_p} - \mathrm{c_m}\right|^2 \qquad (5)$$

The $\underline{R}$ (Eq. (6)) is often used in the linear regression to know how strong is the relationship between the predicted and actual values (Aydin et al., 2018).

$$\mathrm{R} = \frac{\sum(\mathrm{c_p} - \overline{\mathrm{c_p}})(\mathrm{c_m} - \overline{\mathrm{c_m}})}{\sqrt{\sum(\mathrm{c_p} - \overline{\mathrm{c_p}})^2}\sqrt{\sum(\mathrm{c_m} - \overline{\mathrm{c_m}})^2}} \qquad (6)$$

where, C_{m} is the measured value at given time i, $\mathcal{C}_p$ is a predicted particle concentration at the time i and N is the total number of observations, respectively.

A target diagram is used as an additional performance measurement tool to see an extensive response of model that was adopted by the European Commission (Pederzoli et al.,) and the methodology synchronized with statistical pointers within the delta tool (Thunis et al., 2012; Paas et al., 2017). The target diagram explains the MB and CRMSE values, both parameters are stabilized with the help of standard deviation of the observations (σ_{O}), on the ordinate and abscissa, respectively (Pederzoli et al.,) as follow (Eq.(7)) and (Eq.(8)).

$$\mathrm{MB} = \frac{1}{\mathrm{N}}\sum_{\mathrm{i=1}}^{\mathrm{N}}(\mathrm{C_P} - \mathrm{C_M}) = \ \overline{\mathrm{C}}_{\mathrm{P}} - \ \overline{\mathrm{C}}_{\mathrm{M}} \qquad (7)$$

$$\mathrm{CRMSE} = \frac{1}{N}\sqrt{\sum_{i=1}^{N}[(C_P - \bar{C}_P) - (C_M - \bar{C}_M)]^2} \quad (8)$$

For an acceptable model, it must fulfil the criteria of target diagram boundary condition (Eq. (9)); all the outcomes of the model values plotted under circle radius of one and the calculated value of MEF becomes greater than zero. Likewise, if the above two conditions are automatically fulfilled: the normalized MB and MEF values must lie less than or equal to one and the predicted and observed data are positively correlated. Generally, if MEF value is positive, the model has better performance and lower mean square error, whereas the target values is plotted outside the circle and values are negative (Pederzoli et al., 2012).

$$\mathrm{MEF} = 1 - \left(\frac{\mathrm{RMSE}}{\delta O}\right)^2 \quad (9)$$

The FB (Eq. (10)) is an additional performance measurement tool it indicates the basic difference between the predicted and observed data (Cox and Tikvart, 1990).

$$\mathrm{FB} = \frac{2(\bar{C}_M - \bar{C}_P)}{\bar{C}_M + \bar{C}_P} \quad (10)$$

2. Results and discussion

2.1. Comparison of observed data with standards

The monitoring result indicates that the average hourly PM emissions concentrations vary from site to site. The daily 24 hr average PM concentrations of the two particles measured at 15 sites in Addis Ababa are represented as shown in Fig. 5a, b. It shows that pollutant concentrations vary from sites to sites relative to traffic volume and weather data.

As observed in Fig. 5a, the average daily mean concentrations of PM_{10} lie between 54.21 ± 5.81 and 247.36 ± 37.32 µg/m^3. At the two sites (K18 and KM), the average daily PM_{10} concentrations were 54%-65% higher than the standard and other sites were under AQI (2006) limit values (150 µg/m^3) set for 24 hr. However, in all sites, on average, all measured values were 8%-395% higher than the WHO (2005) limit values (50 µg/m^3) for PM_{10}.

As shown in Fig. 5b, the 24-hr mean $PM_{2.5}$ concentrations of the selected area were between 39.59 ± 4.13 and 85.34 ± 11.86 µg/m^3. However, in all sites, the concentrations of $PM_{2.5}$ were higher than AQI (35 µg/m^3) and WHO (25 µg/m^3) standard set for 24 hr mean value. Besides, the difference observed in this study were found to be between 13%-144% and 58%-241%, which is higher than WHO and AQI target value, respectively. These indicate that emissions related to $PM_{2.5}$ have a significant effect on human health (Fan et al., 2009; Pope and Dockery, 1992). This might be due to the non-functionality of an emission controlling system, fuel quality, lack of controlling program, high traffic chocked; road quality, age, and mileage of vehicles are the main reason (Gu et al., 2019; Tarekegn and Gulilat, 2018; Kume et al., 2010). Currently, the urban area is polluted due to high vehicular exhaust emissions, thus highly alleged for a possible negative effect on human health like asthma and other respiratory diseases, exclusively for more vulnerable groups of the people such as elders, kids and people with other health problems (Habeebullah, 2013).

2.2. Comparing the current study with other particulate matter emissions studies

The results of PM_{10} and $PM_{2.5}$ emission levels of the current study (Addis Ababa) were compared with other cities in developing countries (Table 1). In developing countries, particularly cities in Africa air pollution has been severely affected by vehicles in urban areas due to old vehicle's age (Zachariadis et al., 2001), high daily mileage travelled (Batterman et al., 2014), fuel quality and fleet composition (Sternbeck et al., 2002). Moreover, scarce of relevant transport-related data, air pollution controlling and monitoring activity has been given less attention by the higher official and sometimes even used as a political tool to motivate their people and celebrate once a year. Academician also did a little research from higher institute and research center for the fulfillment of their academic requirement on air quality emission, which all of the factors mentioned make getting data in this area challenging. However, here we find and incorporate seven African cities and three other countries (Brazil, India and Pakistan cities) data investigated from 2006 to 2018. The investigators included a single to 16 sites (Table 1).

The PM concentration recorded in the Athi River Township (Kenya), at the three sites ranged from 13.51 to 463.31 µg/m^3 for PM_{10} and 10.3 to 111.23 µg/m^3 for $PM_{2.5}$, which is exceeding the WHO guideline limits of 50 and 25 µg/m^3, respectively. Industrial activities and road traffic considered as the major source in the area (Shilenje et al., 2015). Compared with our result in Athi River Township results showed lower minimum and higher maximum range values of PM_{10} and $PM_{2.5}$ were observed in the later study (Table 1). In the same country, Kenya (at Nairobi city) relatively lower and higher ranges (10.7-128.7 µg/m^3) of $PM_{2.5}$ concentration were also observed in four sites investigated by other

researchers. High road traffic and rural background are the main sources of pollution in the area (Kinney et al., 2011), which is differed to our study roadside traffic emission.

A study conducted in Accra, (Ghana), the 24-hr concentration of PM_{10} and $PM_{2.5}$ ranged from 57.9 to 93.6 µg/m^3 and 22.3 to 40.2 µg/m^3, respectively, which are lower than our study. However, both exceeded the WHO limits in some sites. Road traffic, residential, biomass for small commercial purpose are the main sources of pollution in the city (Arku et al., 2008). A study carried out in Pakistan (Mahar et al., 2013), Egypt (Lowenthal et al., 2014), Algeria (Talbi et al., 2018), and Brazil (Souza et al., 2014) were also showed relatively lower $PM_{2.5}$ and PM_{10} concentrations (Table 1). However, $PM_{2.5}$ and PM_{10} results reported in India (Das et al., 2015), Uganda (Schwander et al., 2014), and Congo (Mbelambela et al., 2017) has been by far greater than the current study (Table 1), suggesting that the intensity of air pollution difference in the four countries.

2.3. Statistical performance measures of the two models

In this study for a better comparison of the models in different road configurations, two intersection road at two sites (National Theater and Kolf-18) and two roundabouts at two sites (Yekatit-12 and Ministry of Education square) were incorporated to see the prediction performance of the two proposed models. The sites are selected arbitrarily from previously collected data for the need for testing and validation of a trained model. The outputs of the two models was tested and validated using unseen input data of the four selected sites and then the result were associated with the observed data. Then, after the prediction performance of Trainlm and Trainscg model were evaluated using the RMSE, MAE, MSE, R^2, MB, MEF, FB value and other statistical parameters as shows in (Table 2).

As shown in Table 2, in all sites, the Trainlm and Trainscg models for PM_{10} R^2 values lie between 0.965 and 0.993 and 0.925 and 0.944, respectively, which is almost approached to 1 in both models. Whereas, the statistical prediction performance of the two models for $PM_{2.5}$ R^2 values range between 0.867 and 0.976 for Trainlm and between 0.392 and 0.845 for Trainscg models. Results of predicted concentrations of PM_{10} in both models show quite approached with the observations over entire sites. However, the predicted concentration of $PM_{2.5}$ values better in only in Trainlm than Trainscg models. Moreover, other statistical conformity, which has listed in Table 2, includes MAE, MSE, and RMSE, the minimum error was observed in Trainlm in both cases. Based on the results, the Levenberg-Marqudrant algorithm has shown a better advantage in terms of accuracy in MAE, MSE, RMSE, and R^2. This clearly shows that the statistical prediction performance of Trainlm neural network models has higher than Trainscg in all areas. Similar to this study finding, other also reported the

outputs of both algorithms were comparable in terms of the correlation coefficient and other statistical parameters (Gardner and Dorling, 1999; Aydin et al., 2018). However, the Scaled Conjugate Gradient Algorithm has better performance in massive data (Mohamad et al., 2010).

In Table 2 FB value have been found -0.043-0.075 for PM_{10} and -0.04-0.05 for $PM_{2.5}$ in both cases the obtained results lay between the expected range. Fractional bias is a supplementary performance measurement the acceptable range between -2 for utmost overestimate, +2 for utmost under-estimate and zero for a perfect model (Chang and Hanna, 2004). The obtained MEF score values of PM_{10} range between 0.92 and 0.99 for Trainlm, 0.83, and 0.88 for Trainscg models. However, the model MEF score values of $PM_{2.5}$ lie between 0.71-0.95 for Trainlm and 0.30-0.71 for Trainscg models. The MEF prediction result is an additional model performance measuring parameters. For this work, the calculated value of MEF was positive and all value is inside under the boundary value (radius = 1) or acceptable limited (Taylor, 2001). For an acceptable model, the outcomes must lie under the boundary circle of the diagram so that the obtained value of the MEF becomes > 0 (Pederzoli et al., 2012).

From Table 3, the stabilized CRMSE score values of $PM_{2.5}$ and PM_{10} lie between 0.013-0.384 for Trainlm and Trainscg models. Whereas, the stabilized MB score values of $PM_{2.5}$ and PM_{10} lie between -0.18-0.081 for Trainlm and Trainscg models. The CRMSE and MB prediction results are an additional model performance measuring parameters. To accept the results, a minimum 90% of the observed sites should fulfilled the target performance indicator of the normalized value of CRMSE and MB is ≤ 1 (Thunis et al., 2012).

2.4. Graphical performance measures of the two models

In this section, the prediction performance of each model was evaluated using a scatter plot and a line chart. As shown in Fig. 6a-h, the predicted value for PM_{10} and $PM_{2.5}$ concentrations has associated with observed data. The solid black and red lines represent the linear regression slope between observations and the forecasting using Trainlm and Trainscg models, for the respective sites. Whereas, the black and red dots indicate the predicted value from the Trainlm and Trainscg models for respective sites and the arrangement of each concentration to their slope. The results of predicted concentrations of PM_{10} from Fig. 6a-d in both models display a better agreement with observations over the entire sites. However, the obtained results of predicted concentrations of $PM_{2.5}$ shown in Fig. 6e-h were found to be the best in Trainlm model. Whereas, in Trainscg except for Fig. 6e at K18 site the rest show somehow a fine

agreement with observations over the whole sites. The poor (R^2 = 0.523) performance of the Trainscg model in K18 site most likely due to the physical reasons of the site. Indeed, K18 is the area more confided and proximity to residence house and service center (such as hotels, roadside fast wood cocker, and road construction activity) than other sampling sites. Moreover, the lower R-value observed for all sites in Trainscg model than Trainlm could be due to a limited data used to predict the concentration of PM. In fact, previous studies indicated that with vast data the Trainscg model showed better performance with accuracy at short time (Batra.D, 2014; Møller, 1993; Mohamad et al., 2010).

As shown in all Fig.7, the black lines indicate the observed (experimental data) for the respective sites. The red lines designate the forecasted values for Trainlm methods in all aspects. Finally, the blue lines specify the forecasted values for Trainscg methods for the respective sites. The graph clearly shows that each model's value outline with the actual data. For the PM_{10} model as shown in Fig. 7a-d in both models the profile almost coincides with the observed data, but still in Trainlm methods has a better fitting than Trainscg. Similarly, Fig. 7e-h shows the graphical performance of $PM_{2.5}$, in this case, the difference is clearly observed between the two models that Trainlm graph is more approach to the observed graph. The better prediction performance outline obtained in Trainlm model. Besides, the graph has also been demonstrated that the pick hours for high PM concentration in the city. As shown in all graphs the pick hours of high concentration is early morning from 6 am to 9 am, then again rise from 11 am, and stay until 7 pm.

As shown in Table 4, the average predicted R^2-values for 15 sites is lying between 0.918-0.993 in Trainlm and 0.863-0.966 in Trainscg models for PM_{10}. Whereas, the predicted R^2-value in all 15 sites for $PM_{2.5}$ lies between 0.867-0.976 in Trainlm and 0.392-0.929 in Trainscg models. However, the overall average predicted R^2-values of the city for PM_{10} are 0.959 for Trainlm and 0.920 in Trainscg. However, R^2-values for $PM_{2.5}$ are 0.943 and 0.775 for Trainlm and Trainscg respectively.

Finally, the air quality model standard performance judging scale range value is not yet decided (Yassin, 2013). Even though there is not a common universally acceptable range, as observed in the figures and tables in this work, the Trainlm model can be considered and satisfactory when most of its forecasting value is more approached to the observations (Chang and Hanna, 2004). Usually, the predicted value closer to the observed value, the actual diagrams approached to at the origin of the target diagram at this point the model performance is improved (Thunis et al., 2012).

3. Conclusions

This work has shown that the levels of transport-related 24 hr average $PM_{2.5}$ and PM_{10} concentrations in 15 sites in Addis Ababa. Thereafter, using artificial neural networks can accurately model the relationship between meteorological, traffic data and $PM_{2.5}$ and PM_{10} concentrations in the urban environment. The experimental result in this study shows that the city average 24-hr $PM_{2.5}$ and PM_{10} emission concentration were greater than the Air quality index and World health organization 24-hr standard limit value. This is maybe because of the vehicle mileage, age, emission treatment technology, fuel quality, driving style, road conjunction and other factors. In this study, the models were seen to learn the underlying pattern of emission without requiring any explicit mathematical representations. This allows easily predicting PM concentration with the Trainlm and Trainscg algorithm training function using an ANN modeling in MATLAB software. Although further detail seasonal variation effect on the ANN model required, various weather conditions such as sunny, cloud, rain and windy recorded during data collection in the study area highlights the potential application of this model at different seasons. The arrangement of the layers is 5-6-1 (number of input layers-hidden layers-outputs layers nodes). The overall results showed that a better correlation coefficient obtained in the Trainlm model, though this method has could be considered as optional methods to predict transport-related particulate matter concentration emission using traffic volume and weather data.

Acknowledgments

We would like to thank Ecole Centrale Nantes, Campus France, and Arba Minch University for the support of testing kits and encouragement to undertake this study. We would like to thank Meteoblue Company in providing online access for meteorological data. Finally, we would like to extend our appreciation to the Office of Addis Ababa Traffic management and its entire traffic police staff for their full cooperation to undertake on-roadside PM sampling.

We would like to thank Mr. Girmaw Tilahun for his continuous support during experimental Campaign. Finally, we would also thank Mr. Shimels Reta for his great diligence during data collection processing phases.

References

Air Quality Sensor: Series 500 Portable Air Monitor Manual, 2018. Aeroqual. Available: https://www.aeroqual.com/product/series-500-portable-air-pollution-monitor. Accessed date: February 18, 2019.

Amaral, S., de Carvalho, J., Costa, M., Pinheiro, C., 2015. An overview of particulate matter measurement instruments. Atmos. 6(9), 1327-1345.

Arku, R.E., Vallarino, J., Dionisio, K.L., Willis, R., Choi, H., Wilson, J.G., et al., 2008. Characterizing air pollution in two low-income neighborhoods in Accra, Ghana. Sci. Total. Environ. 402(2-3), 217-231.

Aydin, M., Yavuz, A., Sorusbay, C., 2018. Application of artificial neural network to predict exhaust emissions from road transport. Int. J. Sci. Technol. Res. 4(2), 1-12.

Batra, D., 2014. Comparison between Levenberg-Marquardt and Scaled Conjugate Gradient training algorithms for image compression using MLP. Int. J. Img. Process. 8(6), 412-422.

Batterman, S., Burke, J., Isakov, V., Lewis, T., Mukherjee, B., Robins, T., 2014. A Comparison of exposure metrics for traffic-related air pollutants: Application to epidemiology studies in Detroit, Michigan. Int. J. Environ. Res. Pub. Health. 11(9), 9553-9577.

Cabaneros, S.M., Calautit, J.K., Hughes, B.R., 2019. A review of artificial neural network models for ambient air pollution prediction. Environ. Model. Softw. 119, 285-304.

Chang, J.C., Hanna, S.R., 2004. Air quality model performance evaluation. Meteorol. Atmos. Phys. 87, 167-196.

Cirak, B., Demirtas, S., 2014. An application of artificial neural network for predicting engine torque in a biodiesel engine. Am. J. Energy. Res. 2(4), 74-80.

Coudray, N., Dieterlen, A., Roth, E., Trouvé, G., 2009. Density measurement of fine aerosol fractions from wood combustion sources using ELPI distributions and image processing techniques. Fuel 88(5), 947-954.

Cox, W.M., Tikvart, J.A., 1990. A statistical procedure for determining the best performing air quality simulation model. Atmos. Environ. A. Gen. Top. 24(9), 2387-2395.

Das, R., Khezri, B., Srivastava, B., Datta, S., Sikdar, P.K., Webster, R.D., et al., 2015. Trace element composition of $PM_{2.5}$ and PM_{10} from Kolkata a heavily polluted Indian metropolis. Atmos. Pollut. Res. 6(5), 742-750.

Fan, Z. (Tina), Meng, Q., Weisel, C., Laumbach, R., Ohman-Strickland, P., Shalat, S., et al., 2009. Acute exposure to elevated $PM_{2.5}$ generated by traffic and cardiopulmonary health effects in healthy older adults. J. Expo. Sci. Environ. Epidemiol. 19(5), 525-533.

Gardner, M.W., Dorling, S.R., 1999. Neural network modelling and prediction of hourly NOx and NO_2 concentrations in urban air in London. Atmos. Environ. 33(5), 709-719.

Gardner, M.W., Dorling, S.R., 1998. Artificial neural networks (the multilayer perceptron) a review of applications in the atmospheric sciences. Atmos. Environ. 32(14-15), 2627-2636.

Garg, B.D., Cadle, S.H., Mulawa, P.A., Groblicki, P.J., Laroo, C., Parr, G.A., 2000. Brake wear particulate matter emissions. Environ. Sci. Technol. 34(21), 4463-4469.

Habeebullah, T.M., 2013. Health impacts of PM_{10} using AirQ2.2.3 Model in Makkah. J. Basic Appl. Sci. 9, 259-268.

Hamanaka, R.B., Mutlu, G.M., 2018. Particulate matter air pollution: Effects on the cardiovascular system. Front. Endocrinol. 9, 680.

Hung-Lung, C., Yao-Sheng, H., 2009. Particulate matter emissions from on-road vehicles in a freeway tunnel study. Atmos. Environ. 43(26), 4014-4022.

Keil, C., Kassa, H., Brown, A., Kumie, A., Tefera, W., 2010. Inhalation exposures to particulate matter and carbon monoxide during Ethiopian coffee ceremonies in Addis Ababa: A pilot study. J. Environ. Pub. Health. 2010, 8.

Kermani, B.G., Schiffman, S.S., Nagle, H.T., 2005. Performance of the Levenberg–Marquardt neural network training method in electronic nose applications. Sensors and Actuators B: Chem. 110(1), 13-22.

Kinney, P.L., Gichuru, M.G., Volavka-Close, N., Ngo, N., Ndiba, P.K., Law, A., et al., 2011. Traffic impacts on $PM_{2.5}$ air quality in Nairobi, Kenya. Environ. Sci. Policy. 14(4), 369-378.

Kume, A., Charles, K., Berehane, Y., Anders, E., Ali, A., 2010. Magnitude and variation of traffic air pollution as measured by CO in the city of Addis Ababa, Ethiopia. Ethiop. J. Health. Dev. 24(3).

Lowenthal, D.H., Gertler, A.W., Labib, M.W., 2014. Particulate matter source apportionment in Cairo: Recent measurements and comparison with previous studies. Int. J. Environ. Sci. Technol. 11 (3), 657-670.

Mahar, A., Ahmad, I., Malik, N., Gabol, W.A., Channa, S.A., Shah, S.N.M., et al., 2013. Concentrations of road transport-related air pollutants and its health implications of Hyderabad City, Pakistan. Global. J. Environ. Sci. Manag. 3(2), 269-275.

Maier, H.R., Jain, A., Dandy, G.C., Sudheer, K.P., 2010. Methods used for the development of neural networks for the prediction of water resource variables in river systems: Current status and future directions. Environ. Model. Softw. 25(8), 891-909.

Mbelambela, E.P., Hirota, R., Eitoku, M., Muchanga, S.M.J., Kiyosawa, H., Yasumitsu-Lovell, K., et al., 2017. Occupation exposed to road-traffic emissions and respiratory health among Congolese transit workers, particularly bus conductors, in Kinshasa: a cross-sectional study. Environ. Health Prev. Med. 22(1), 11.

Meiller, M.F., 1991. Original contribution a scaled conjugate gradient algorithm for fast supervised learning. Neural Netw. 6(4), 525-533.

Mitike, G., Motbainor, A., Kumie, A., Samet, J., Wipfli, H., 2016. Review of policy, regulatory, and organizational frameworks of environment and health in Ethiopia. Ethiop. J. Health. Dev. 30(1), 42–49.

Mohamad, N., Zaini, F., Johari, A., Yassin, I., Zabidi, A., 2010. Comparison between Levenberg-Marquardt and Scaled Conjugate Gradient training algorithms for breast cancer diagnosis using MLP. In 2010 6th Int. Colloquium on Signal. Process. Appl. 1-7. IEE.

Møller, M.F., 1993. A scaled conjugate gradient algorithm for fast-supervised learning. Neural Netw. 6(4), 525-533.

A., Agrawal, M., 2017. A Global perspective of fine particulate matter pollution and its health effects. Rev. Environ. Contam. Toxic. 244. Springer, Cham. 5-51.

Ngo, N.S., Asseko, S.V.J., Ebanega, M.O., Allo'o, S.M.A., Hystad, P., 2019. The relationship among $PM_{2.5}$, traffic emissions, and socioeconomic status: Evidence from Gabon using low-cost, portable air quality monitors. Transp. Res. D. 68, 2-9.

Paas, B., Stienen, J., Vorländer, M., Schneider, C., 2017. Modelling of urban near-road atmospheric PM concentrations using an artificial neural network approach with acoustic data input. Environ. 4(2), 26.

Padoan, E., Amato, F., 2018. Vehicle non-exhaust emissions: impact on air quality. In: Non-Exhaust Emissions. Acad. Press, 21-65.

Pant, P., Harrison, R.M., 2013. Estimation of the contribution of road traffic emissions to particulate matter concentrations from field measurements: A review. Atmos. Environ. 77, 78-97.

Park, S., Kim, M., Kim, M., Namgung, H.-G., Kim, K.-T., Cho, K.H., et al., 2018. Predicting PM_{10} concentration in Seoul metropolitan subway stations using artificial neural network (ANN). J. Hazard. Mater. 341, 75-82.

Pederzoli, A., Thunis, P., Georgieva, E., Borge, R., Carruthers, D., Pernigotti, D., 2012. Performance criteria for the benchmarking of air quality model regulatory applications: the 'target' approach. Int. J. Environ. Pollut. 50(1-4), 175-189.

Penkała, M., Ogrodnik, P., Rogula-Kozłowska, W., 2018. Particulate matter from the road surface abrasion as a problem of non-exhaust emission control. Environ. 5(1), 9.

Pope, C.A., Dockery, D.W., 1992. Acute health effects of PM_{10} pollution on symptomatic and asymptomatic children. Am. Rev. Respir. Dis. 145(5), 1123-1128.

Ropkins, K., Beebe, J., Li, H., Daham, B., Tate, J., Bell, M., et al., 2009. Real-world vehicle exhaust emissions monitoring Review and critical discussion. Crit. Rev. Environ. Sci. Technol. 39(2), 79-152.

Schwander, S., Okello, C.D., Freers, J., Chow, J.C., Watson, J.G., Corry, M., et al., 2014. Ambient Particulate Matter Air Pollution in Mpererwe District, Kampala, Uganda: A Pilot Study. J. Environ. Pub. Health. 2014.

Shilenje, Z., Thiong'o, K.T., Ondimu, K.I., Nguru, P.M., Nguyo, J., Ongoma, V., et al., 2015. Ambient air quality monitoring and audit over Athi River Township, Kenya. Int. J. Sci. Res. Environ. Sci. 3(8), 291–301.

Souza, D.Z., Vasconcellos, P.C., Lee, H., Aurela, M., Saarnio, K., Teinilä, K., et al., 2014. Composition of $PM_{2.5}$ and PM_{10} Collected at Urban Sites in Brazil. Aerosol Air Qual. Res. 14(1), 168-176.

Stafoggia, M., Faustini, A., 2018. In Book: Chapter 3 - Impact on public health epidemiological studies: A review of epidemiological studies on non-exhaust particles: Identification of gaps and future needs, Non-exhaust emissions. Acad. Press, 67-88.

Sternbeck, J., Sjödin, Å., Andréasson, K., 2002. Metal emissions from road traffic and the influence of resuspension results from two tunnel studies. Atmos. Environ. 36(30), 4735-4744.

Suratgar, A.A., Tavakoli, M.B., Hoseinabadi, A., 2007. Modified Levenberg-Marquardt method for neural networks training .World Acad. Sci. Eng. Technol. 6(1), 46-48.

Talbi, A., Kerchich, Y., Kerbachi, R., Boughedaoui, M., 2018. Assessment of annual air pollution levels with PM1, $PM_{2.5}$, PM_{10} and associated heavy metals in Algiers, Algeria. Environ. Pollut. 232, 252-263.

Tarekegn, M.M., Gulilat, T.Y., 2018. Trends of ambient air pollution and the corresponding respiratory diseases in Addis Ababa. Res. Rep. Toxi. 2(1), 5.

Taylor, K.E., 2001. Summarizing multiple aspects of model performance in a single diagram. J. Geophys. Res. Atmos. 106(D7), 7183-7192.

Tefera, W., Asfaw, A., Gilliland, F., Kumie, A., Worku, A., 2014. Indoor and outdoor air pollution- related health problem in Ethiopia: Review of related literature. Ethiop. J. Health .Dev. 30(1), 5-16.

Thunis, P., Georgieva, E., Pederzoli, A., 2012. A tool to evaluate air quality model performances in regulatory applications. Environ. Model. Softw. 38, 220-230.

Timmers, V.R.J.H., Achten, P.A.J., 2016. Non-exhaust PM emissions from electric vehicles. Atmos. Environ. 134, 10-17.

US EPA, O., 2016. Particulate Matter (PM) Basics. Available: https://www.epa.gov/pm-pollution/particulate-matter-pm-basics. Accessed date: June 5, 2020.

Watson, A.Y., Bates, R.R., Kennedy, D., 1988. Automotive emissions, air pollution, the automobile, and public health. National Acad. Sci. Eng. Med. 704.

Winkler, S.L., Anderson, J.E., Garza, L., Ruona, W.C., Vogt, R., Wallington, T.J., 2018. Vehicle criteria pollutant (PM, NOx, CO, HCs) emissions: how low should we go? N.P.J. Clim. Atmos. Sci. 1(1), 1-5.

Xue, H., Jiang, S., Liang, B., 2013. A study on the model of traffic flow and vehicle exhaust emission. Math. Probl. Eng. 2013.

Yassin, M.F., 2013. Numerical modeling on air quality in an urban environment with changes of the aspect ratio and wind direction. Environ. Sci. Pollut. Res. 20(6), 3975-3988.

Zachariadis, T., Ntziachristos, L., Samaras, Z., 2001. The effect of age and technological change on motor vehicle emissions. Transp. Res. D. Transp. Environ. 6(3), 221-227.

Table1. Shows the range of 24 hr-mean PM_{10} and $PM_{2.5}$ concentrations levels obtained from this study and other developing country.

Study area			Concentrations (µg/m^3)		Periods	Site description	Reference
Place	**Country**	**# Site**	**PM_{10}**	**$PM_{2.5}$**			
Addis Ababa	Ethiopia	15	54.2-247.4	39.6-85.3	Oct. to Nov., 2018	Road traffic	This study
Athi RT	Kenya	3	13.5-463.3	10.3-111.2	Dec., 2014 to Jan., 2015	Industrial and road traffic	(Shilenje et al., 2015).
Nairobi	Kenya	4	NR	10.7-128.7	Jul., 2009	Road traffic and rural background	(Kinney et al., 2011)
Accra	Ghana	4	57.9-93.6	22.3-40.2	Jun. to Jul., 2006	Residential and traffic site	(Arku et al., 2008)
Kampala	Uganda	1	132.7-208.1	103.7-104.9	Dec., 2012 to Jan., 2013	Urban background and traffic	(Schwander et al., 2014).
Kolkata	India	16	167.0-928.0	83.0-783.0	Dec. 2013 to Jan., 2014	Road traffic, construction, and industrial	(Das et al., 2015),
Kinshasa	Congo	4	NR	64.2-128.7	Apr. to May, 2015	Road-traffic	(Mbelambela et al., 2017)
Hyderabad	Pakistan	5	40.0-117.0	NR	Dec. to Jan., 2013	Road traffic, industrial, and background	(Mahar et al., 2013)
Cairo	Egypt	5	104.0-184.0	32.0-58.0	May to Oct., 2010	Road traffic, industrial, and background	(Lowenthal et al., 2014)
Algiers	Algeria	2	15.5-121.6	9.4-84.7	Jan., 2015 to Nov., 2016	Roadside, urban and industrial	(Talbi et al., 2018)
Sao Paulo	Brazil	2	9.0-39.0	6.0-83.0	Aug. to Nov., 2008	Road traffic, industrial, and agricultural	(Souza et al., 2014)

0 RT: River Township, NR: Not Reported

Table 2. Artificial Neural Network model statistical performance for PM_{10} and $PM_{2.5}$ concentration the values of the selected sites.

		@ K18 site		PM_{10} @ NT site		@ MOE site		@ Y12 site	
Model	**PM**	Trainlm	Trainscg	Trainlm	Trainscg	Trainlm	Trainscg	Trainlm	Trainscg
MAE	10	16.34	53.78	3.71	13.96	5.34	10.48	4.50	7.86
	2.5	10.27	36.21	4.30	13.71	3.42	7.44	5.51	6.23
MSE	10	832.88	4202.04	29.10	292.78	154.89	229.65	44.47	154.29
	2.5	245.21	2385.45	63.76	371.07	23.04	104.24	48.14	71.33
RMSE	10	28.86	64.82	5.39	17.11	12.45	15.15	6.67	12.42
	2.5	15.66	48.68	7.99	19.26	4.80	10.21	6.94	8.45
R^2	10	0.99	0.93	0.99	0.92	0.96	0.94	0.98	0.93
	2.5	0.963	0.523	0.976	0.845	0.947	0.732	0.867	0.392
FB	10	-0.043	0.001	-0.015	-0.017	-0.032	0.075	0.020	-0.044
	2.5	-0.03	-0.04	0.04	0.00	0.02	0.05	-0.01	0.03
MEF	10	0.97	0.87	0.99	0.86	0.92	0.88	0.95	0.83
	2.5	0.93	0.30	0.95	0.71	0.89	0.52	0.76	0.64
SD' ($\mu g/m^3$)	10	178.79	178.79	45.2	45.2	43.1	43.1	29.91	29.91
	2.5	58.11	58.11	35.61	35.61	14.74	14.74	14.15	14.15
SD ($\mu g/m^3$)	10	173.91	154.66	46.27	44.48	46.56	39.11	32.53	34.12
	2.5	53.51	35.31	36.11	35.07	14.00	11.52	12.50	11.51
C_M ($\mu g/m^3$)	10	231.72	231.7	76.56	76.56	80.29	80.29	54.29	54.29
	2.5	85.34	85.34	50.50	50.50	57.31	57.31	44.54	44.54
C_P ($\mu g/m^3$)	10	241.8	231.34	77.78	77.95	82.91	74.48	53.22	56.73
	2.5	87.58	88.95	48.62	50.58	56.10	54.66	45.10	43.10

LM; Levenberg-Marquardt, SCG: Scaled Conjugate Gradient, SD': Standard Deviations of observations, SD: Standard Deviation of predictions CM: mean concentration of observations, and CP Mean concentrations of Predictions.

Table 3. Stabilized centralized mean square error and mean bias tabulated for target diagram.

	$PM_{10}(CRMSE/\sigma_O)$		$PM_{2.5}(CRMSE/\sigma_O)$		$PM_{10}(MB/\sigma_O)$		$PM_{2.5}(MB/\sigma_O)$	
Model	Trainlm	Trainscg	Trainlm	Trainscg	Trainlm	Trainscg	Trainlm	Trainscg
K18	0.027	0.089	0.078	0.384	0.056	-0.002	0.039	0.062
NT	0.043	0.023	0.013	0.015	0.026	0.030	-0.053	0.002
Y12	0.086	0.052	0.114	0.182	-0.036	0.081	0.039	-0.108
MOE	0.079	0.169	0.049	0.214	0.061	-0.135	-0.083	-0.180

Table 4. Summary of obtained results from the model for 24-hr concentrations.

Model R value	Trainlm		Trainscg	
Area code	PM_{10}	$PM_{2.5}$	PM_{10}	$PM_{2.5}$
ATS	0.955	0.951	0.895	0.845
JMS	0.932	0.923	0.897	0.700
KM	0.926	0.937	0.863	0.823
KGM	0.967	0.966	0.911	0.734
K18	0.988	0.963	0.931	0.523
LM	0.974	0.961	0.942	0.891
MDS	0.918	0.940	0.910	0.711
MES	0.956	0.959	0.925	0.929
MS	0.931	0.938	0.896	0.866
MES-1	0.975	0.959	0.941	0.867
MOE	0.965	0.947	0.944	0.732
NT	0.993	0.976	0.925	0.845
THS	0.962	0.925	0.925	0.921
TD	0.965	0.933	0.966	0.841
Y12	0.980	0.867	0.933	0.392

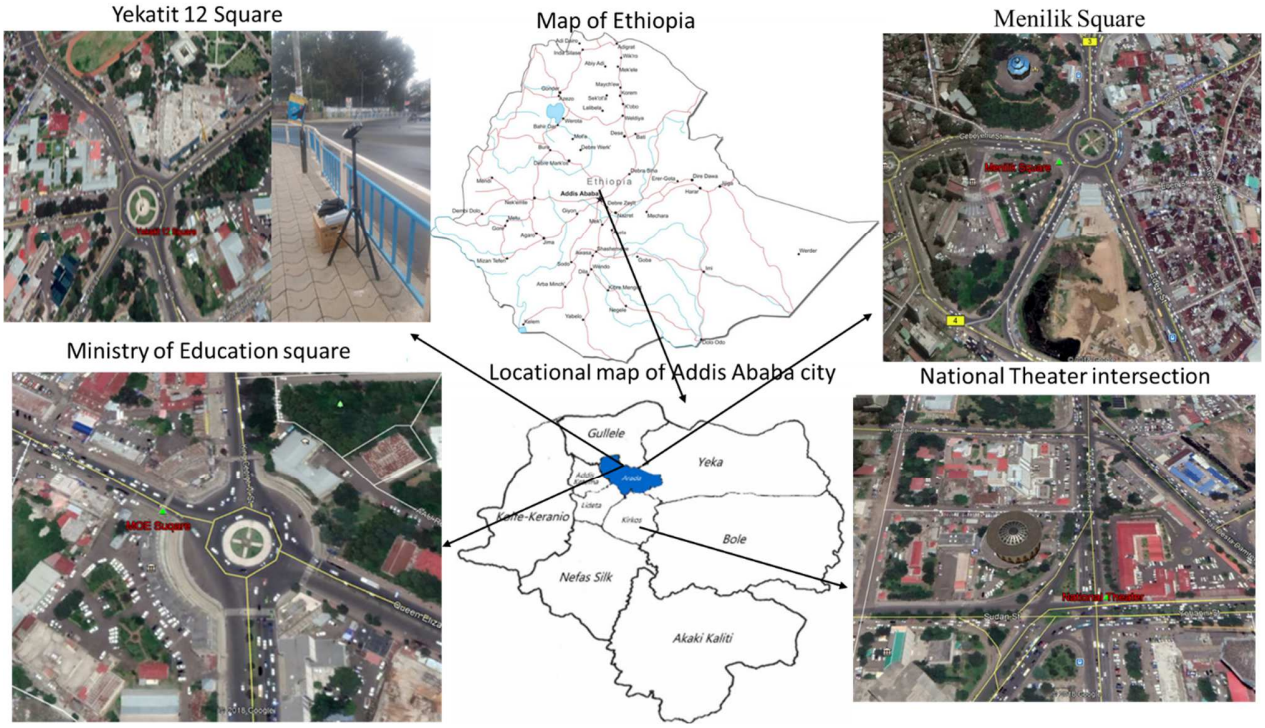

Fig.1. Study area and monitoring sites.

.

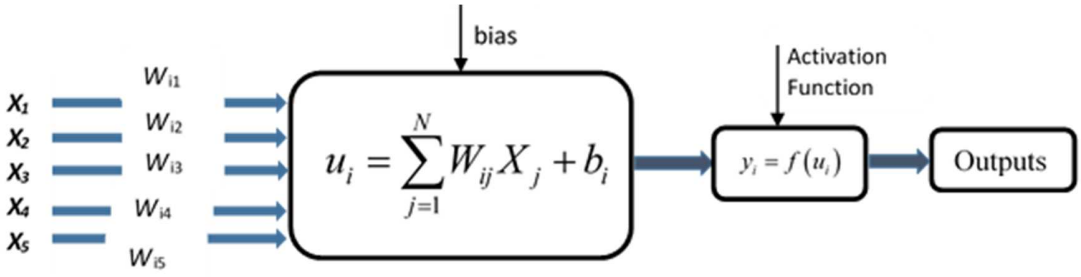

Fig. 2. A non-linear model of neural computation.

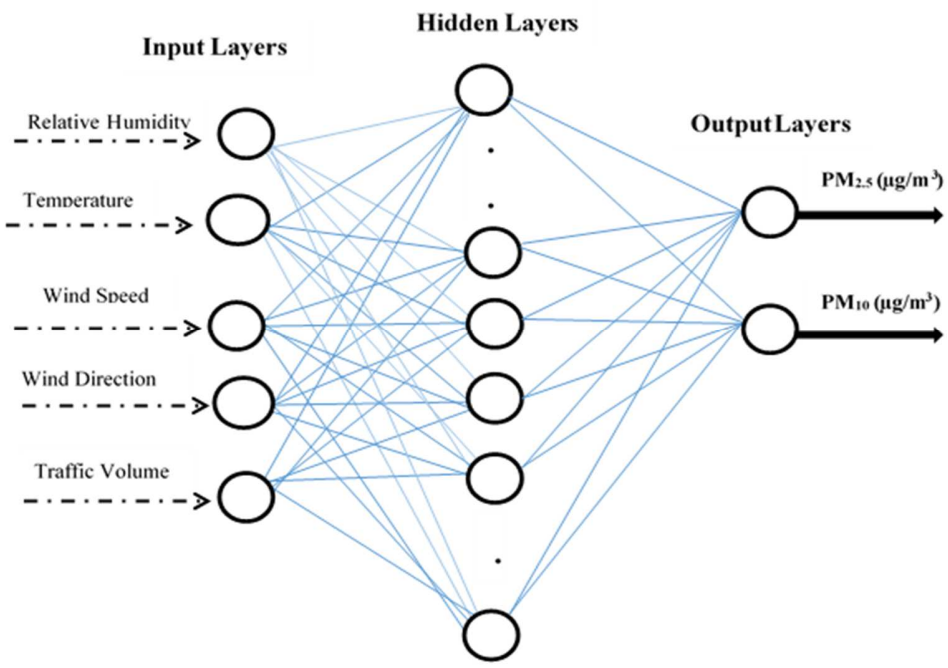

Fig. 3. Architecture of the proposed artificial neural network model.

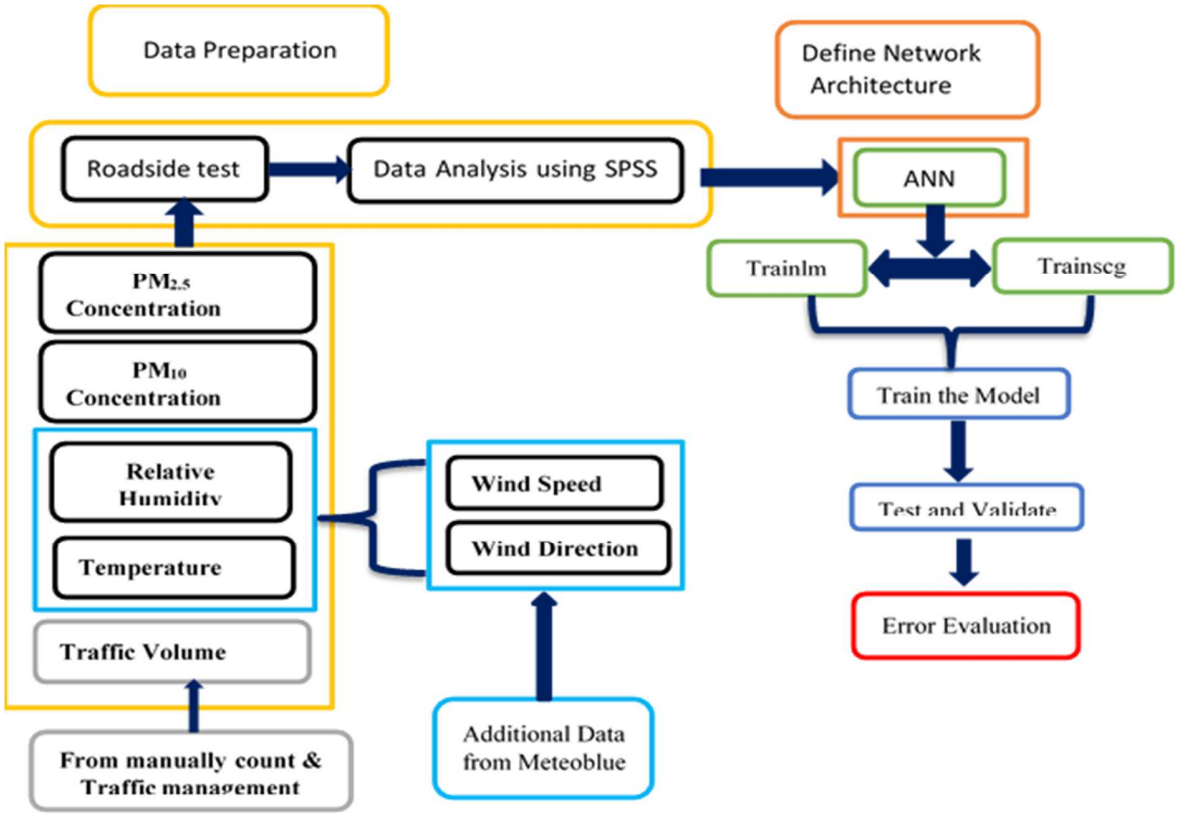

Fig. 4. Quality assurance and workflow for the proposed model.

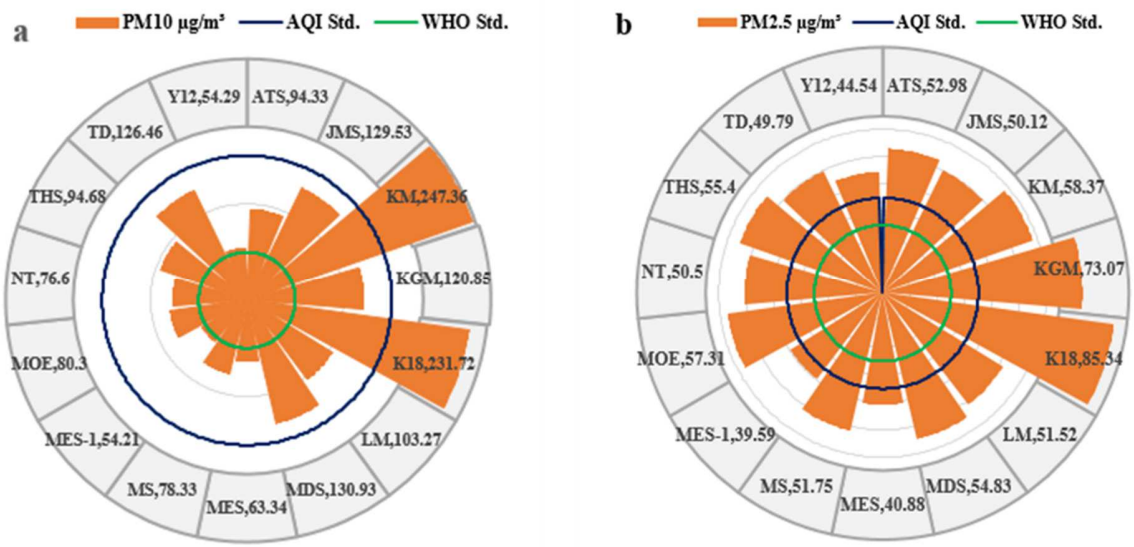

Fig. 5. Radar chart 24 hr average PM_{10} ($\mu g/m^3$) (a) and $PM_{2.5}$ ($\mu g/m^3$) (b) concentrations at 15 sites.

ATS: Ayer Tena Square (ATS), JMS: Jemo Michael Intersection, KM: Kaliti Maseltegna, KGM: Kera-Gofa Mazoria, K18: Kolfa 18, LM: Lafto-Mebrate, MDS: Megenagna Diaspora Square, MS: Meskel Square, MS: Menilik Square, MSE1: Meskel Square -1, MOE: Ministry of education square, NT: National Theater, THS: Torhyloch square, TD: Tulu Dimtu, and Y12: Yekatit 12 Square.

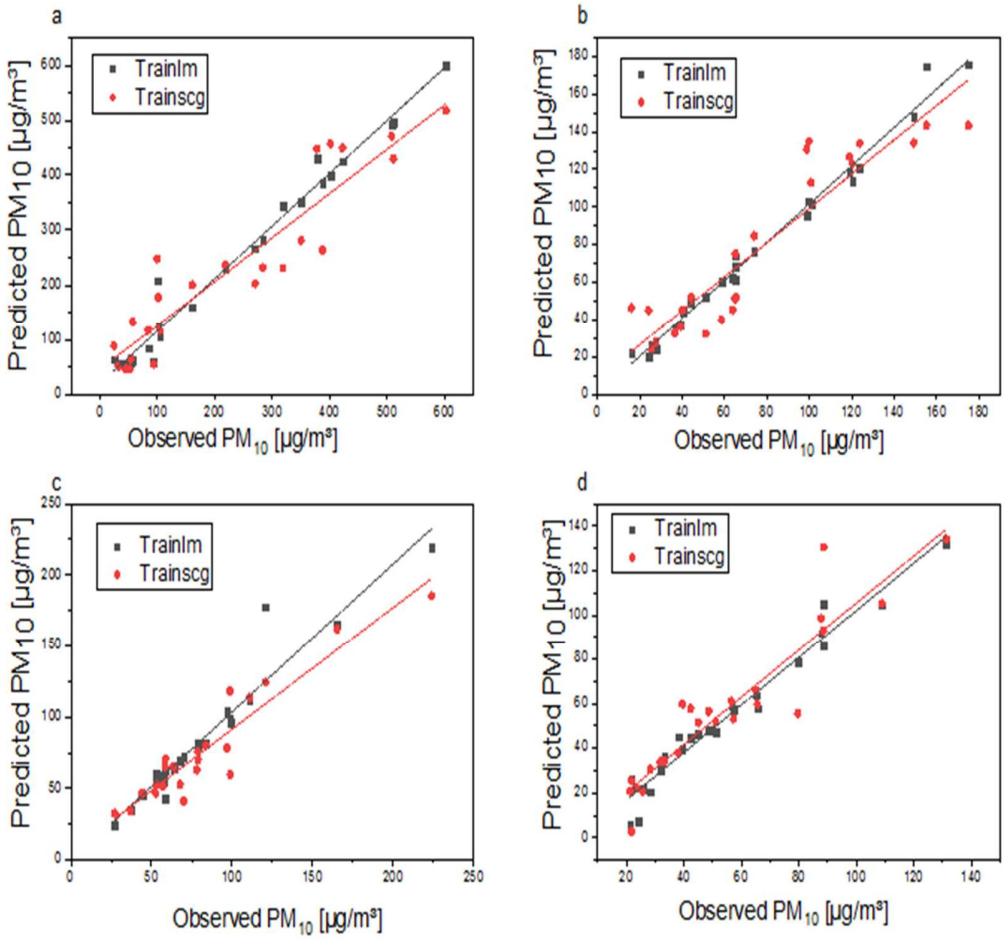
a
Predicted PM10 [µg/m³]
Observed PM10 [µg/m³]
Trainlm
Trainscg
b
Predicted PM10 [µg/m³]
Observed PM10 [µg/m³]
Trainlm
Trainscg
c
Predicted PM10 [µg/m³]
Observed PM10 [µg/m³]
Trainlm
Trainscg
d
Predicted PM10 [µg/m³]
Observed PM10 [µg/m³]
Trainlm
Trainscg

Cont. Fig. 6

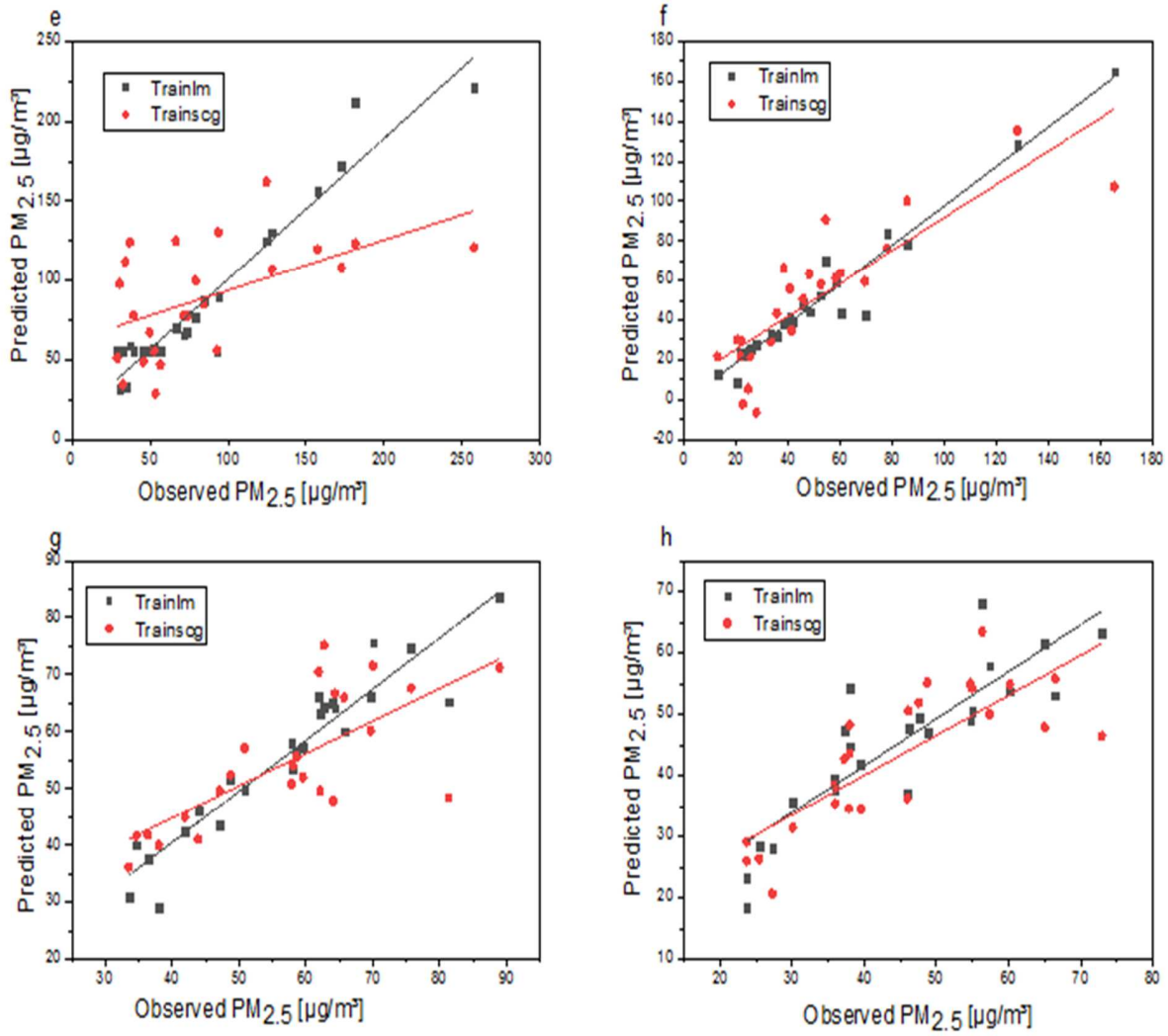

Fig.6. Scatter plot diagrams show the two artificial neural network model predictions of PM_{10} (a - d) and $PM_{2.5}$ (e- h) concentrations for (a and e) K18 site, (b and f) for NT site, (c and g) for MOE site and (d and h) for Y12 sites.

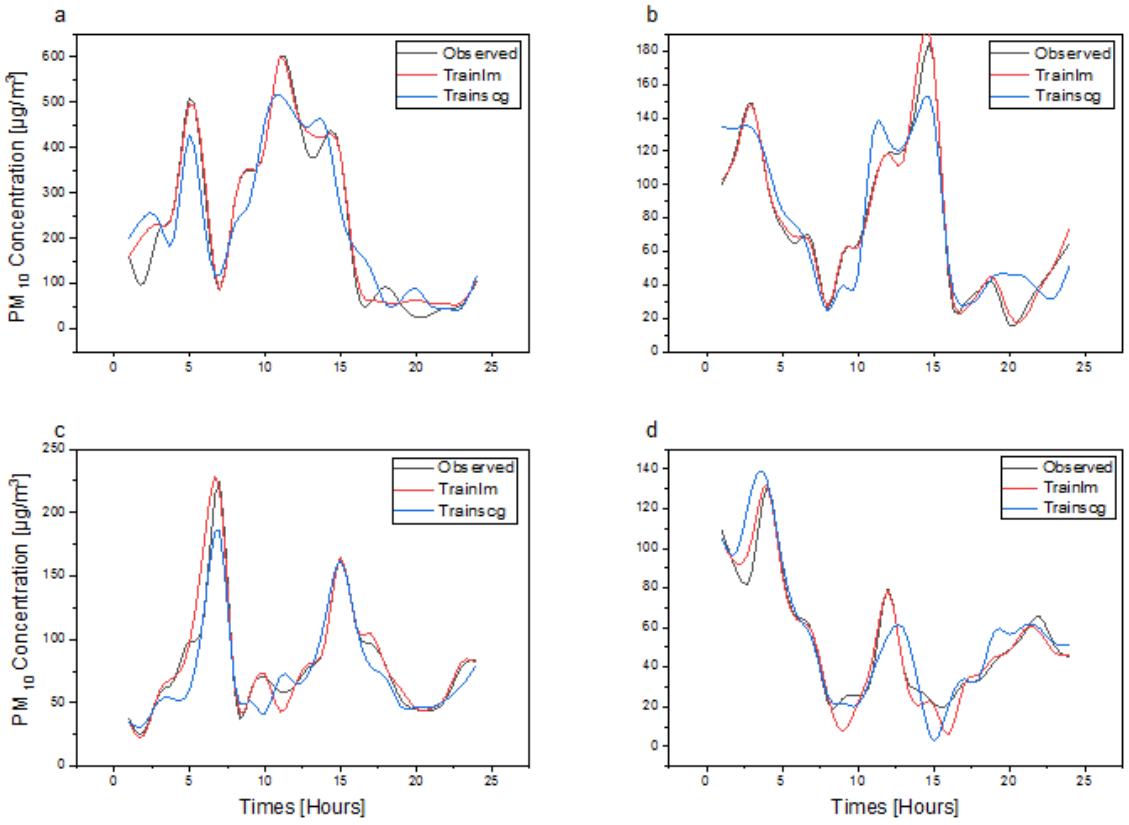
a
b
c
d
Observed
Trainlm
Trainscg
PM 10 Concentration [µg/m³]
Times [Hours]

Cont. Fig. 7

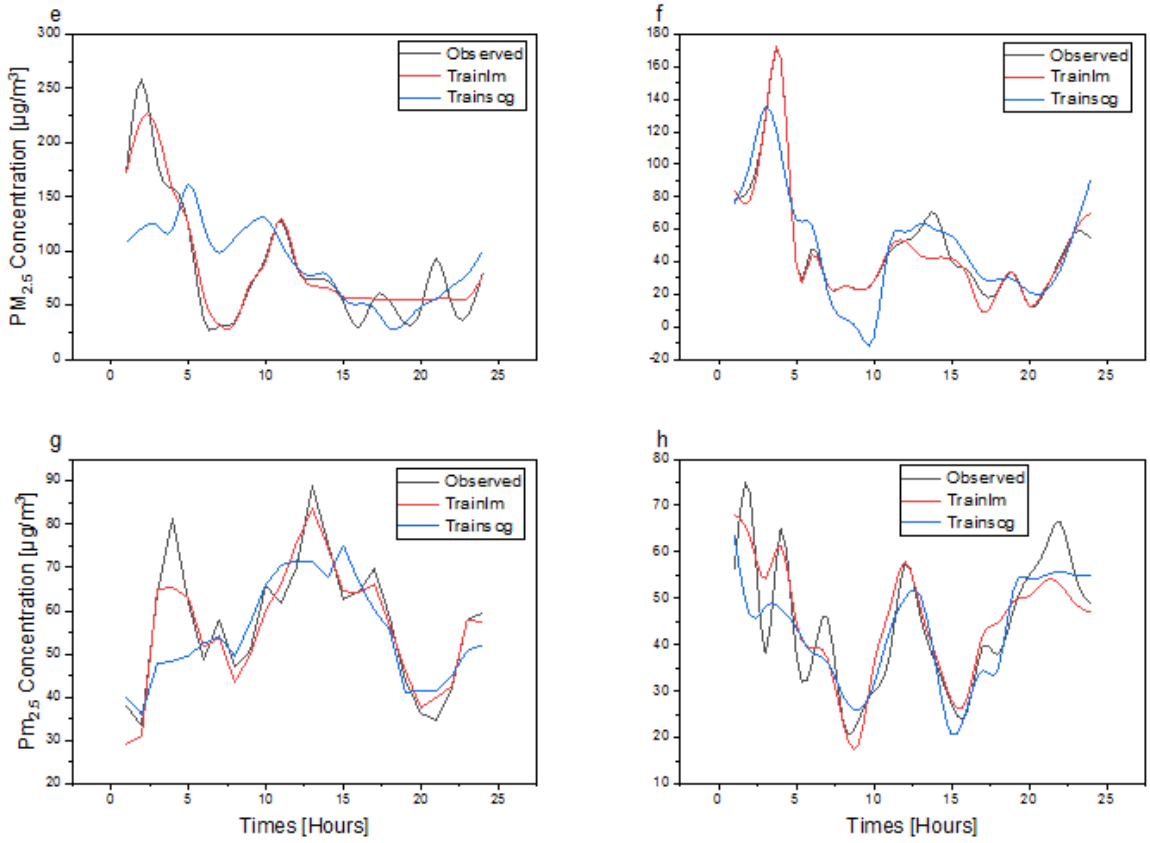

Fig. 7. Observed and Predicted PM_{10} (a-d) and $PM_{2.5}$ (e-h) concentration for 24 hr at K18, NT, MOE, and Y12 sites, respectively.